

Supporting Information for:

Ganglioside-Lipid and Ganglioside-Protein Interactions Revealed by Coarse-Grained and Atomistic Molecular Dynamics Simulations

Ruo-Xu Gu[†], Helgi I. Ingólfsson[‡], Alex H. de Vries[‡], Siewert J. Marrink[‡], D. Peter Tieleman^{*†}

[†]Centre for Molecular Simulation and Department of Biological Sciences, University of Calgary, 2500 University Drive, N.W., Calgary, Alberta T2N 1N4, Canada

[‡]Groningen Biomolecular Sciences and Biotechnology (GBB) Institute and Zernike Institute for Advanced Materials, University of Groningen, Nijenborgh 7, 9747 AG Groningen, The Netherlands

Bilayer properties of the atomistic and CG simulations: Different water models and treatments of electrostatic interactions have effects on the bilayer properties at the CG level, including the bilayer thickness, area per lipid, lipid order parameters, and lipid diffusion coefficients, as shown in Table S1. Using PW makes the bilayer shrink and results in a smaller area per lipid, larger bilayer thickness, and higher order parameters. However, calculating the long-range electrostatic interactions with PME makes the bilayer expand. The diffusion coefficients of lipids are decreased significantly in the CG PW simulations, particularly for the GM lipids, whereas the corresponding values are increased with PME. In all of the CG simulations, the diffusion coefficients of GM lipids are smaller than POPC lipids, whereas the values of GM3 are larger than GM1. The aggregation of GM lipids may be the reason of the smaller diffusion coefficients of GM lipids. The lipid diffusion coefficients in the atomistic simulations are significantly smaller than the values in the CG simulations. The CG diffusion coefficients reported in Table S1 are based on the simulation time, i.e., we do not rescale them based on effective time. The smoother energy landscape at the CG level results in much faster dynamics, hence the difference in atomistic and CG diffusion coefficients is in the range of 5-10 fold. Lower diffusion was found for the POPC lipids in the upper leaflet compared with those of the lower leaflet, due to coupling with the GM lipids.

Densities of water molecules, POPC lipids, gangliosides, as well as ganglioside headgroups along the membrane normal are shown in Fig.S2. Densities profiles of the CG and atomistic simulations match well with each other, with minor differences. The ganglioside headgroups extend further into the water layer in the atomistic simulations than in the CG simulations (Fig. S2).

The order parameters of GM lipids are increased (ca. 0.31 and 0.41 in the simulations using the original and new force fields, respectively, Table S1), because of the changes of bond lengths of AM1-AM2, and AM2-T1A. However, there are still notable differences of the GM chain order parameters between the CG newFF and the atomistic simulations, suggesting the necessity of optimizing the parameters of the Martini ceramide building blocks but this is outside the scope of this work. The differences between the atomistic and CG GM lipid order parameters may also be responsible for the smaller area per lipid (APL) at the atomistic level. The diffusion coefficients of GM lipids with the new force field are also increased

significantly, due to the weaker interactions between them, as shown in Table S1. The density profiles of POPC lipids, gangliosides, and each sugar of the ganglioside headgroups in the simulations using the optimized force field are also calculated (Fig. S9). The distributions of the sugars in ganglioside headgroups are shifted to the solution a little, particular for the sugar Gal. In simulations with the original Martini force field, the density profiles of Gal overlap with those of the POPC headgroup, whereas in the simulations with modified parameters, the Gal density profiles are located in solution, which is in better agreement with the atomistic simulations (Fig. S2 and S9).

Re-optimization of angle and dihedral parameters of Martini ganglioside force field:

Angles and dihedrals involved in the orientation of the headgroups are modified, specifically, dihedral *GM3-GM1-AM1-AM2* is removed, new parameters are used for angle *GM3-GM1-AM1*, and a new angle *GM2-GM1-AM1* is added (Fig. 7 and Table S3). Distributions of angles and dihedrals that are affected by these changes are shown in Fig. S5. Angles and dihedrals involved in the relative orientations of the sugars are also modified slightly. Most of the changes are the same for lipid GM1 and lipid GM3, as shown in Table S3. Two angles (*GM6-GM13-GM14*, and *GM9-GM10-GM12*) and two dihedrals (*GM5-GM6-GM7-GM8*, and *GM5-GM6-GM7-GM9*) are added for lipid GM1 in order to control the relative orientations of Gal, GalNAc, and Neu5Ac (i.e., the relative orientations of two branches of the headgroup, Fig. 7). However, angle *GM6-GM13-GM14* is not included in lipid GM3. This angle is used to modify the relative orientation between Gal and Neu5Ac, but the relative orientation between them are different in lipid GM1 and lipid GM3, due to the lack of GalNAc-Gal2 groups in lipid GM3. The other angle and dihedrals are not applicable to lipid GM3. For the other changes, and distributions of the angles and dihedrals affected by these changes, see Table S3 and Fig. S6.

Table S1. Bilayer properties of GM-POPC binary mixtures^a.

Simulations		Thk ^b (Å)	APL (Å ²)	Order parameter ^c			Diffusion coefficient ($\times 10^{-8}$ cm ² /s)		
				GM lipids	POPC upper leaflet	POPC lower leaflet	GM lipids	POPC upper leaflet	POPC lower leaflet
GM1	CG W	39.0±0.4	64.4±0.8	0.31±0.04	0.37±0.02	0.38±0.02	13.6±3.7	33.6±1.0	82.4±16.8
	CG PW	39.6±0.4	63.9±0.8	0.32±0.04	0.38±0.02	0.39±0.02	3.0±1.2	8.9±0.3	42.6±1.2
	CG PW PME	39.2±0.4	64.8±0.8	0.30±0.04	0.36±0.02	0.38±0.02	7.9±3.8	16.6±5.3	61.2±8.0
	AA	39.8±0.5	61.2±0.9	0.53±0.04	0.39±0.02	0.42±0.02	3.5±0.2	3.5±0.6	7.9±1.0
	CG W newFF	39.5±0.3	63.6±0.7	0.41±0.04	0.39±0.02	0.39±0.02	20.4±3.3	38.4±4.2	57.9±6.6
	CG PW newFF	40.3±0.3	62.8±0.7	0.42±0.04	0.40±0.02	0.40±0.02	11.5±1.4	19.3±2.0	42.8±6.6
GM3	CG W	39.2±0.4	64.2±0.7	0.30±0.04	0.38±0.02	0.39±0.02	16.6±7.7	37.8±11.3	72.3±1.7
	CG PW	39.7±0.4	63.6±0.7	0.31±0.04	0.38±0.02	0.39±0.02	11.8±2.8	22.1±0.2	49.5±3.6
	CG PW PME	39.4±0.4	64.6±0.8	0.30±0.04	0.37±0.02	0.38±0.02	15.7±2.8	29.5±1.6	54.1±1.7
	AA	39.5±0.5	61.8±0.8	0.55±0.04	0.38±0.02	0.41±0.02	2.8±1.0	4.3±0.8	8.0±0.7
	CG W newFF	39.6±0.4	63.6±0.7	0.42±0.04	0.38±0.02	0.39±0.02	37.7±9.4	47.1±2.1	60.3±0.6
	CG PW newFF	40.2±0.3	63.0±0.7	0.42±0.04	0.40±0.02	0.40±0.02	25.3±4.2	31.3±0.6	44.9±3.7

^a Abbreviations: Thk, bilayer thickness; APL, area per lipid; CG W, CG simulations with the standard Martini water; CG PW, CG simulations with the polarizable Martini water; CG PW PME, CG simulations with the polarizable Martini water in which PME is used for long-range electrostatic interactions; AA, atomistic simulations; CG W newFF, CG simulations with the standard Martini water using the re-optimized force field of gangliosides; CG PW newFF, CG simulations with the polarizable Martini water using the re-optimized force field of gangliosides.

^b For the CG simulations, the bilayer thickness is defined as the distance along the membrane normal between the centers of mass of PO4 beads in two leaflets; for the atomistic simulations, the atoms corresponding to the PO4 beads in the CG simulations are used.

^c For the CG simulations, the order parameters are calculated based on the angle between the bonds of the lipid tails and the bilayer normal (approximated as the box z axes), and are averaged over all tail bonds, lipids and simulation time; for the atomistic simulations, the order parameters are calculated based on the pseudo-CG trajectories. Values are shown as average \pm standard deviation, except for diffusion coefficients where the fit error is reported by the GROMACS tool `g_msdl`.

Table S2. Average number of lipid contacts in the atomistic GM1-GM3-POPC ternary mixture simulation. The trajectory was divided into four blocks and the average and standard deviation were calculated for each block.

lipids	0-0.5 μ s	0.5-1.0 μ s	1.0-1.5 μ s	1.5-2.0 μ s
GM1-GM1	1540 \pm 750	1775 \pm 693	1920 \pm 701	1480 \pm 732
GM3-GM3	935 \pm 835	2550 \pm 892	3036 \pm 714	3207 \pm 1089
GM1-GM3	2275 \pm 610	2154 \pm 556	1822 \pm 378	1537 \pm 585
GM1-POPC	13043 \pm 561	12970 \pm 679	13460 \pm 673	13692 \pm 850
GM3-POPC	12885 \pm 696	12298 \pm 716	12392 \pm 608	12038 \pm 687

Table S3. Modifications of the bond, angle and dihedral parameters of ganglioside headgroups. The parameters of the original and new force fields are compared. The parameters which are different in the original and new force fields are labeled in red.

Bonds	Equilibrium values (nm)		Force Constants (kJ/(mol nm ²))		Angles	Equilibrium Values (degree)		Force constants (kJ/(mol rad ²))		Dihedrals	Equilibrium values (degree)		Force constants (kJ/(mol rad ²))	
	Original FF	New FF	Original FF	New FF		Original FF	New FF	Original FF	New FF		Original FF	New FF	Original FF	New FF
<i>GM1-GM2^a</i>	0.360	0.375	17500	const.	<i>GM2-GM3-GM4</i>	85.5	80	320	350	<i>GM1-GM2-GM3-GM4</i>	-160	-177	30	100
<i>GM1-GM3^a</i>	0.310	0.330	20000	const.	<i>GM3-GM4-GM5</i>	67	60	550	550	<i>GM2-GM3-GM4-GM5</i>	-149	-140	16	16
<i>GM4-GM5^a</i>	0.389	0.396	const.	const.	<i>GM4-GM6-GM7</i>	102	110	350	320	<i>GM3-GM4-GM5-GM6</i>	-150	-159	55	55
<i>GM4-GM6^a</i>	0.300	0.265	const.	const.	<i>GM6-GM7-GM8</i>	57	67.5	700	700	<i>GM4-GM6-GM7-GM8</i>	157	148	180	160
<i>GM7-GM8^a</i>	0.57	0.521	const.	const.	<i>GM6-GM7-GM9</i>	90	102	670	670	<i>GM5-GM6-GM7-GM9</i>	--	5	--	25
<i>GM9-GM10^a</i>	0.300	0.364	const.	const.	<i>GM4-GM6-GM13</i>	97.5	103	295	295	<i>GM5-GM6-GM7-GM8</i>	--	65	--	25
<i>GM10-GM11^a</i>	0.395	0.395	const.	const.	<i>GM6-GM13-GM15</i>	71	67	700	700	<i>GM4-GM6-GM13-GM15</i>	-124	-124	60	55
<i>GM10-GM12^a</i>	0.270	0.268	const.	const.	<i>GM6-GM13-GM14^b</i>	--	133	--	30	<i>GM5-GM4-GM6-GM7</i>	-126	-118	90	90
<i>GM13-GM14^a</i>	0.35	0.35	const.	const.	<i>GM7-GM6-GM13</i>	68.5	68.5	880	880	<i>GM5-GM4-GM6-GM13</i>	154	159	115	125
<i>GM13-GM15^a</i>	0.381	0.381	const.	const.	<i>GM7-GM9-GM10</i>	76	76	290	290	<i>GM6-GM7-GM8-GM9</i>	150	168	32	50
<i>GM14-GM15^a</i>	0.364	0.367	const.	const.	<i>GM9-GM10-GM11</i>	69	73	630	600	<i>GM6-GM13-GM15-GM14</i>	107.5	97.5	265	265
<i>GM2-GM3</i>	0.315	0.327	8500	12000	<i>GM9-GM10-GM12</i>	--	62	--	200	<i>GM7-GM9-GM10-GM11</i>	-156	-128	23	23
<i>GM3-GM4</i>	0.368	0.352	15000	35000	<i>GM13-GM15-GM17</i>	96	100	210	210	<i>GM8-GM7-GM9-GM10</i>	179	152	115	120
<i>GM5-GM6</i>	0.307	0.318	25000	30000	<i>GM15-GM14-GM16</i>	61	58	300	400	<i>GM9-GM10-GM11-GM12</i>	-163	-157	80	80
<i>GM6-GM7</i>	0.36	0.331	11000	11000	<i>GM3-GM1-AM1</i>	50	142	200	50	<i>GM13-GM15-GM14-GM16</i>	137	137	80	80
<i>GM6-GM13</i>	0.376	0.366	12500	25000	<i>GM2-GM1-AM1^c</i>	--	88/ 94	--	25/ 45	<i>GM14-GM13-GM15-GM17</i>	162	159	50	50
<i>GM7-GM9</i>	0.364	0.345	17500	25000	<i>GM1-AM1-AM2</i>	85	65	25	20	<i>GM3-GM2-AM1-AM2</i>	125	--	10	--
<i>GM8-GM9</i>	0.37	0.320	10000	12000										
<i>GM11-GM12</i>	0.32	0.320	12000	12000										
<i>GM14-GM16</i>	0.340	0.340	11500	12500										
<i>GM15-GM17</i>	0.275	0.275	8500	8500										
<i>GM1-AM1</i>	0.57	0.48	20000	8000										
<i>AM1-AM2</i>	0.27	0.37	20000	8500										
<i>AM1-T1A</i>	0.29	0.47	20000	8500										

^a Constraints are applied.

^b Not included in GM3.

^c Different parameters for GM1 and GM3. Equilibrium value and force constant are 88 degree and 25 kJ/(mol rad²) for GM1, whereas the corresponding values are 94 degree and 45 kJ/(mol rad²) for GM3, respectively.

Figure S1. Orientation restraint in GM3-AQP1 PMF calculation. Point *a* is the center of mass of AQP1, whereas point *b* is the center of mass of one AQP1 subunit (AQP1 is a homo-tetramer). The angle θ was restrained at 75 degree by PLUMED to force GM3 to approach AQP1 in one specific direction. The PMF was calculated as a function of the distance *d* between the centers of mass of GM3 and AQP1.

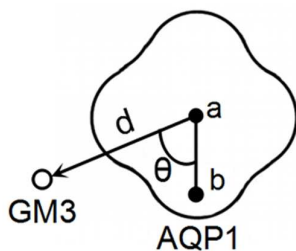


Figure S2. Density profiles of water, POPC, GM lipids, GM headgroups, and each sugar of GM headgroups along the membrane normal.

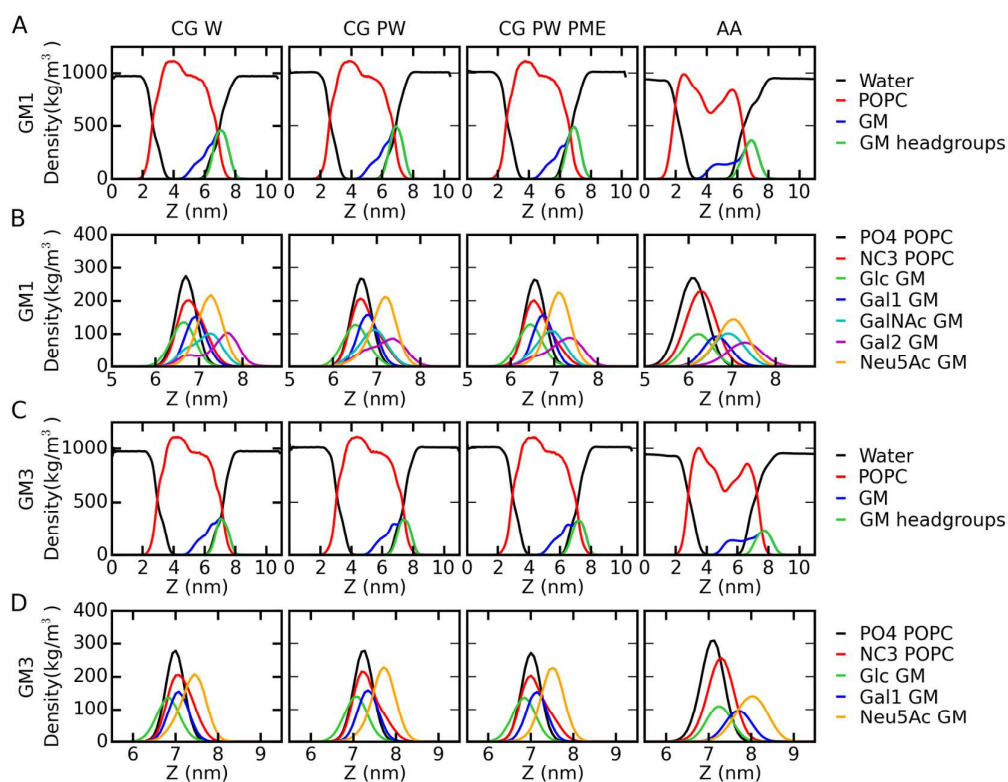


Figure S3. Convergence of the RDF profiles. The RDFs of the gangliosides in both the CG simulation of (A) GM1-POPC binary mixture (PW PME simulation), and the atomistic simulations of (B) GM1-POPC and (C) GM3-POPC binary mixtures are shown as examples.

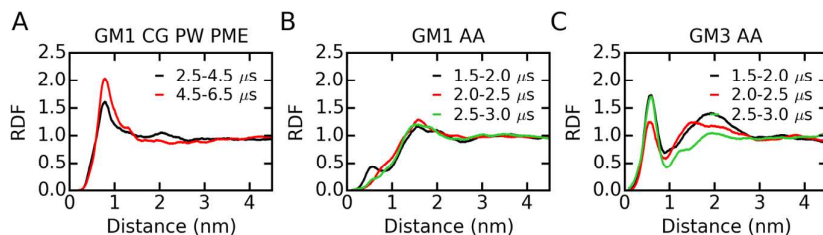


Figure S4. Number of lipid contacts in the atomistic GM1-GM3-POPC ternary mixture simulation. Average contacts between (A) GM lipids (B) ganglioside headgroups, (C) ganglioside tails, and (D) GM lipids to POPC lipids are shown.

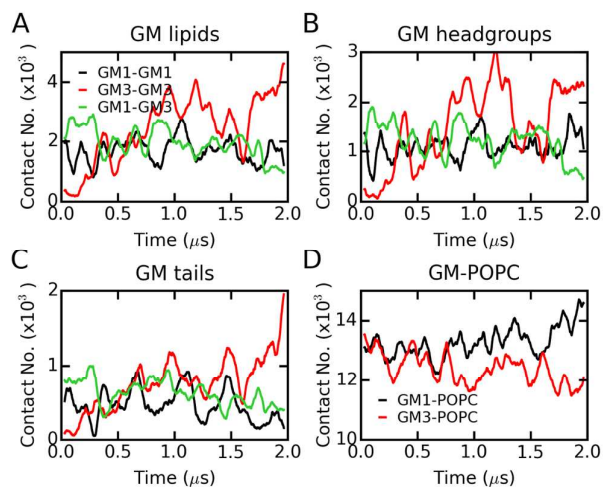


Figure S5. Distributions of angles and dihedrals involved in headgroup orientations of the (A) GM1 and (B) GM3 lipids. All of the angles and dihedrals affected by the changes in the new force field are listed. The results of the CG W simulations are shown. The results of the CG PW and the CG PW PME simulations are similar with those of the CG W simulations.

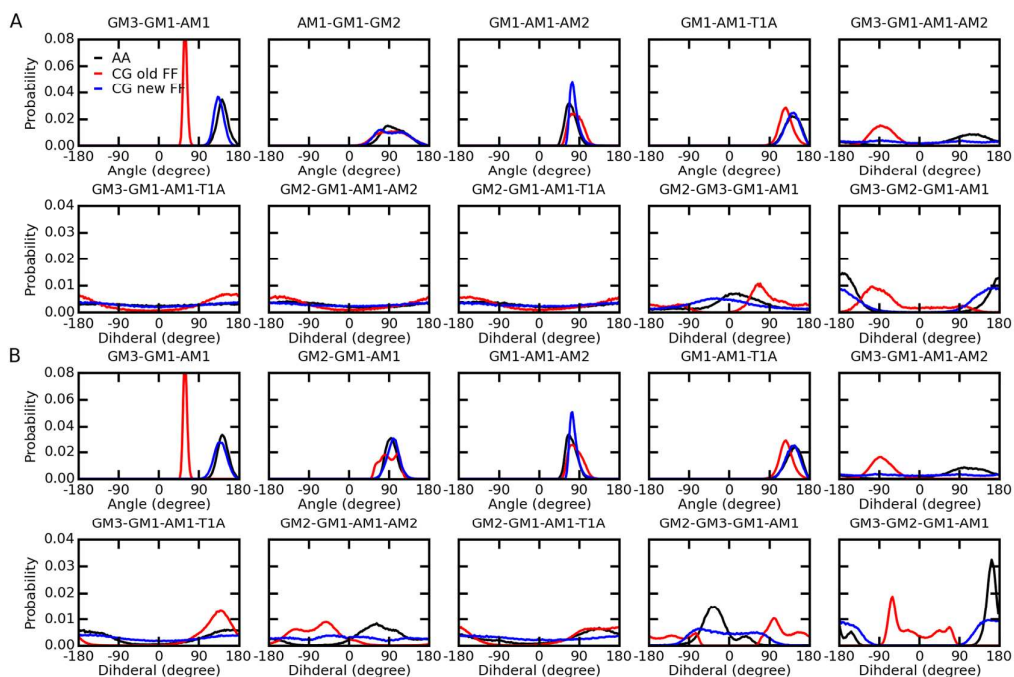


Figure S6. Distributions of angles and dihedrals involved in the relative orientations of the sugars in the headgroups of the (A) GM1 and (B) GM3 lipids. All of the angles and dihedrals affected by the changes in the new force field are listed. The results of the CG W simulations are shown. The results of the CG PW and the CG PW PME simulations are similar with those of the CG W simulations.

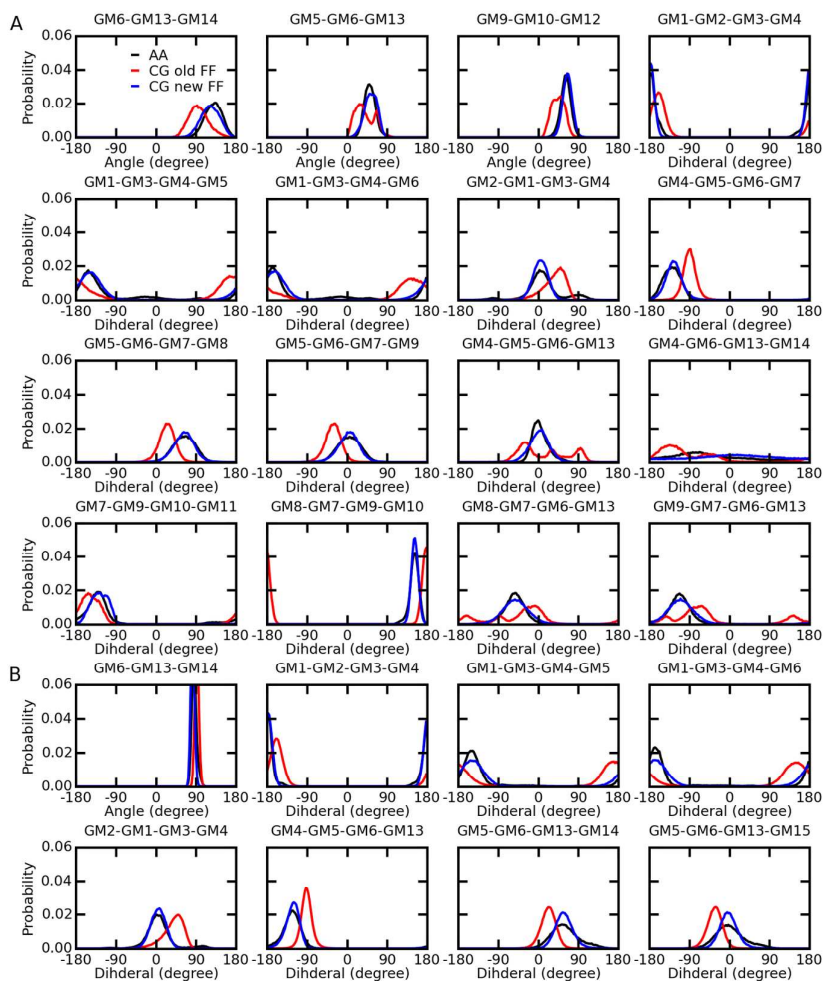


Figure S7. Radial distribution functions (RDFs) between each sugar in the headgroups of the (A) GM1 and (B) GM3 lipids. For the CG simulations, the results of the simulations with standard Martini water model are shown.

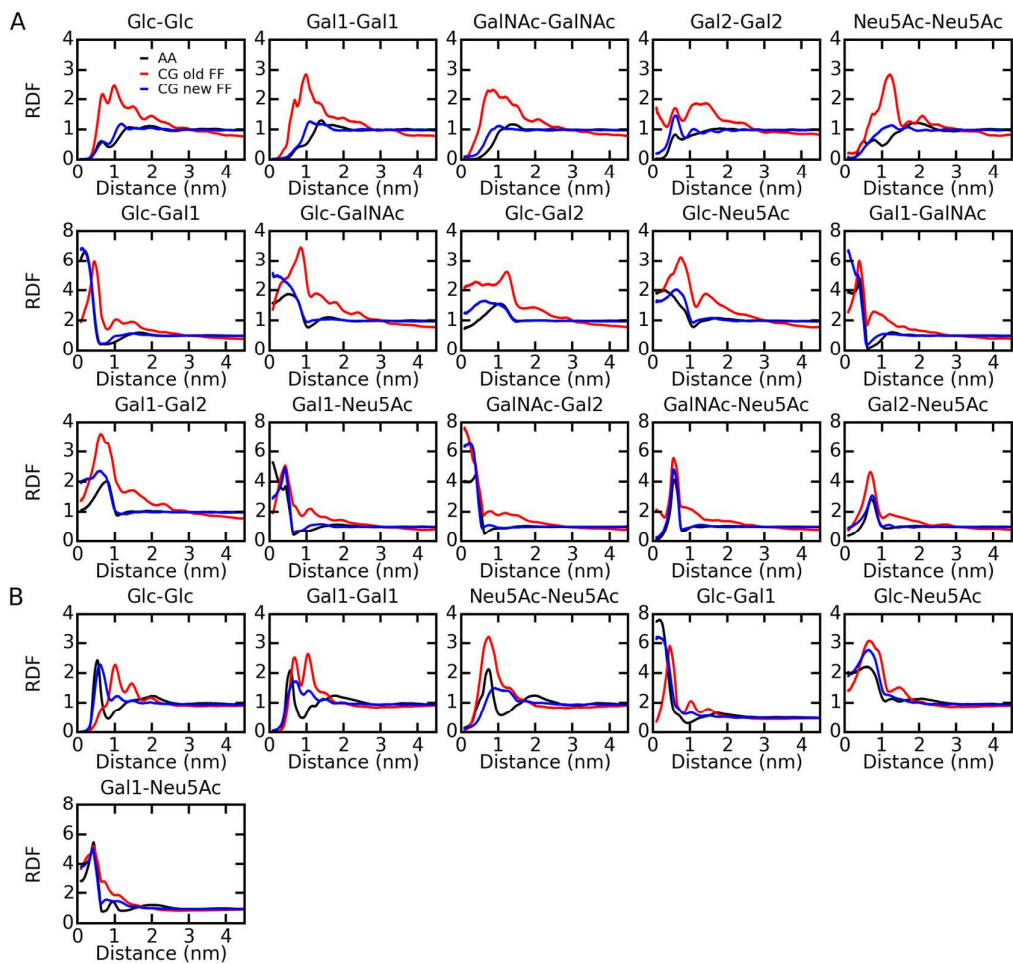


Figure S8. Radial distribution functions (RDFs) between specific CG beads of the headgroups of the (A) GM1 and (B) GM3 lipids. For the CG simulations, the results of the simulations with the standard Martini water model are shown.

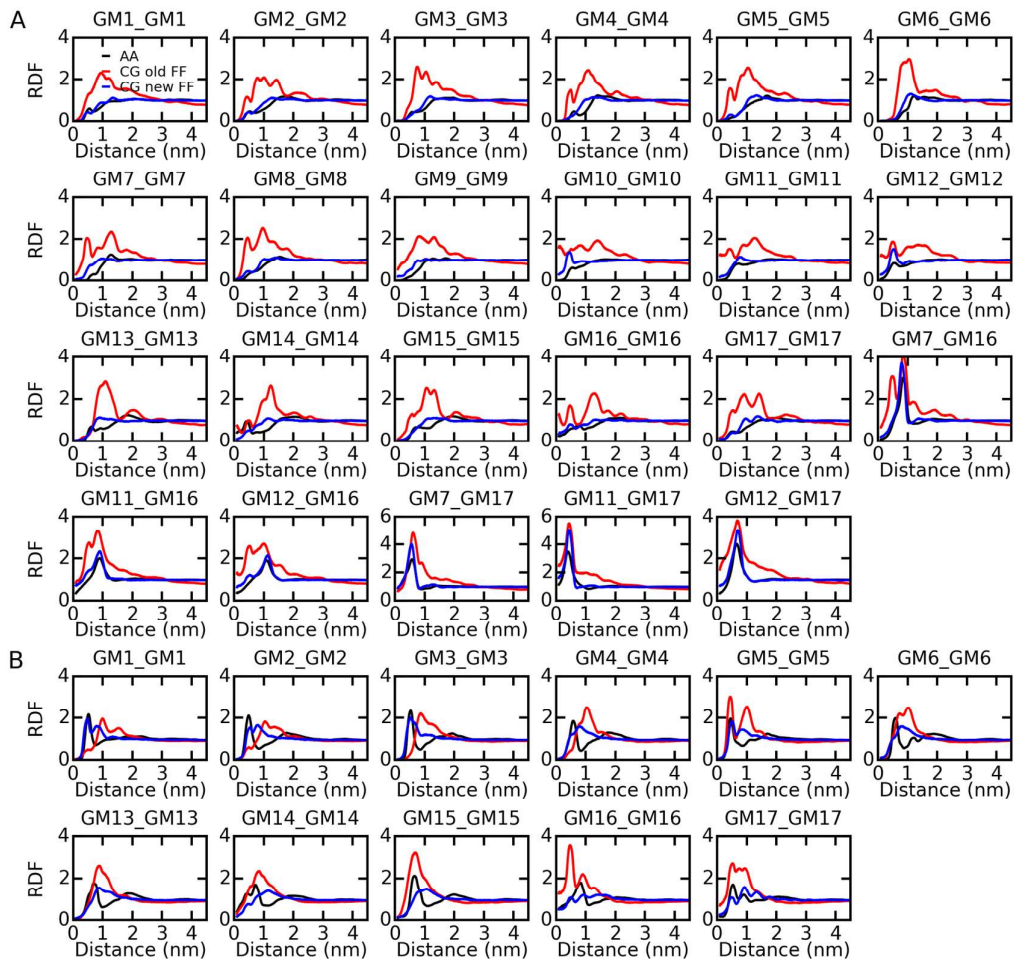


Figure S9. Density profiles of water, POPC, GM lipids, GM headgroups, and each sugar of GM headgroups along membrane normal in the simulations of GM-POPC binary mixtures using the optimized ganglioside force field.

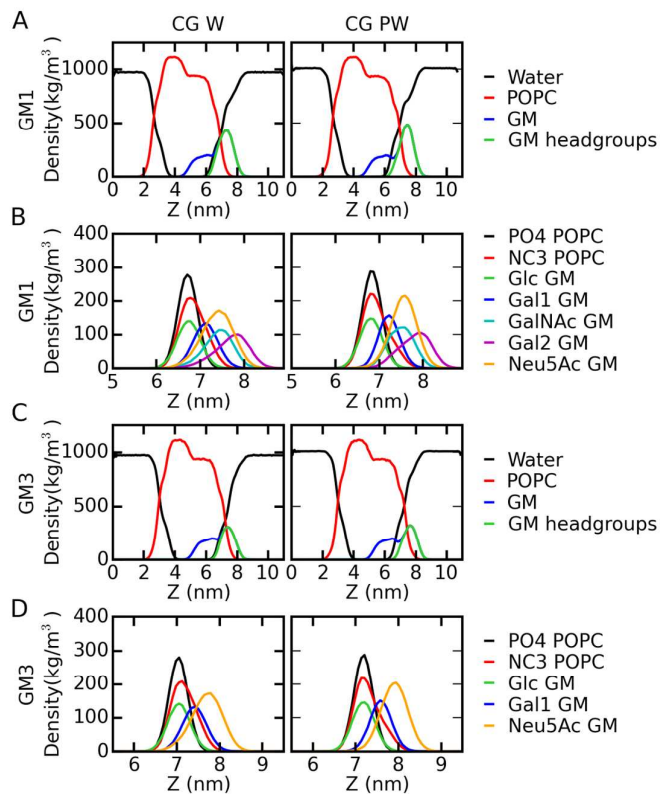


Figure S10. Positions AQP1 charged residues. Positively charged residues (Lys, Arg) and negatively charged residues (Glu, Asp) are shown in magenta and orange, respectively. Only the residues at the upper leaflet are shown. Subunit 1 of AQP1 and the headgroups of GM3 are shown in white and light green, respectively.

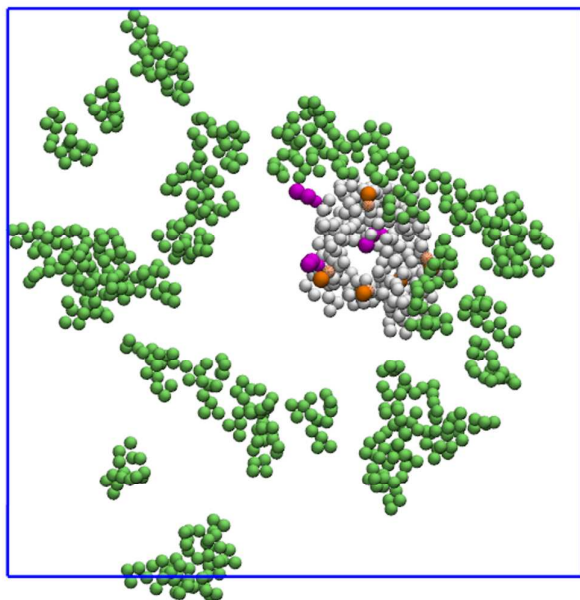


Figure S11. CG W simulations of GM3-POPC mixture at 330 K. (A) Simulations of DPG3-POPC (GM3 lipids with shorter tails) and (B) DBG3-POPC (GM3 lipids with longer tails) bilayers using the original Martini ganglioside force field. (C) Simulation of DBG3-POPC bilayer using the new Martini ganglioside force field. The left column shows the average sizes and numbers of GM3 clusters as a function of simulation time. The right column is the RDFs between the centers of mass of GM3 lipids, GM3 headgroups, GM3 tails, and GM3 and POPC.

